Proceedings of 3rd International Civil Engineering and Architecture Congress (ICEARC'23)
DOI 10.31462/icearc.2023.hyd401

High and low group and monotonic trends of monthly precipitation in the near future (2030-2059) for Bursa province, Türkiye, under the SSP5-8.5 scenario

Murat Şan[1*], Sinan Nacar[2], Murat Kankal[3], Adem Bayram[4]

[1] Gümüşhane University, Department of Civil Engineering, Gümüşhane, Türkiye
[2] Tokat Gaziosmanpaşa University, Department of Civil Engineering, Tokat, Türkiye
[3] Bursa Uludağ University, Department of Civil Engineering, Bursa, Türkiye
[4] Karadeniz Technical University, Department of Civil Engineering, Trabzon, Türkiye

Abstract

Purpose: To determine high and low group and monotonic trends of monthly total precipitation in Bursa Province, which has one of the densest populations in Türkiye, under a pessimistic socio-economic scenario, SSP5-8.5, to examine intra-term changes offering an opportunity to research the details of climate change as well as to study the future changes according to observations.
Study design/methodology/approach: 14 general circulation models (GCMs) from the CMIP6 archive were utilized as input variables for the established multivariate adaptive regression splines based statistical downscaling model at the Bursa meteorological station. This was carried out to generate daily total precipitation for two specific time terms: the near past (1979-2014) and the near future (2030-2059) under the SSP5-8.5. A subset of four high-performance GCMs was selected, and multi-model averages of precipitation were computed to mitigate uncertainties arising from GCMs. Daily totals were converted to monthly totals after correction for possible biases. Intra-term trends were analysed using the innovative trend significance test (ITST) for monotonic trends and improved visualization of innovative trend analysis (IV-ITA) for high and low group trends.
Findings: Total monthly precipitation is projected to decrease by 10 mm (14%) in the near future compared to the near past, with the highest decrease (~24%) in December. According to the ITST results, there is an increasing trend in Feb, Jun, Aug, Sep, and Oct during the near past term, while a decreasing trend is projected in the near future and vice versa for Jan and Nov. To the IV-ITA results, while an increasing trend is generally observed in the range of 11-50% (28-84%) of low (high) values in Jan, Feb, Aug, and Sep (Feb, Jun, Aug, Sep, and Oct) during the near past term, a decreasing trend is predicted in the range of 34-100% (28-61%) in the near future. However, different direction trends emerged for low and high values in Jan, Jun, and Dec, both in the near past and near future.
Originality/value: In this study, in addition to comparing future and past monthly precipitation, trend changes in high and low groups were analysed with innovative methods.

Keywords: CMIP6 Archive, Improved Visualization, Innovative Trend Analysis, Precipitation, SSP5-8.5

* Corresponding author (muratsan@gumushane.edu.tr)
© 2023 Authors. Publishing services by golden light publishing®.
This is an open-access article under the CC BY-NC-ND license (http://creativecommons.org/licenses/by-nc-nd/4.0/).

1. Introduction

Climate change is the long-term alteration in climate variability and averages, persisting for over a decade. This phenomenon is one of the most critical challenges affecting humanity and the environment. The frequency, intensity, and duration of disasters such as floods, droughts, heatwaves, and forest fires steadily increase with climate change (Ahmed et al., 2018; Şan et al., 2023). The repercussions of this global change are also experienced at regional levels, with the Mediterranean Basin, including Türkiye, being identified among the most vulnerable regions (Diffenbaugh and Giorgi, 2012; Keupp et al., 2019). Examining the potential impacts of climate change at a regional scale and proactively identifying these effects provide local policymakers with valuable insights for effective decision-making in water resource management.

Global-scale general circulation models (GCMs) are commonly employed to assess the prospective effects of climate change. However, due to their coarse spatial resolutions, GCMs fail to represent regional climatic patterns adequately. Consequently, the downscaling of coarse-resolution models necessitates applying dynamic and statistical downscaling (SD) models. Dynamic downscaling methods entail high computational costs and expert knowledge, whereas SD methods offer a cost-effective, rapid, and easily applicable alternative across diverse regions. Hence, SD methods are frequently preferred in the literature for climate change effect assessments (Ekstrom et al., 2015; Nacar et al., 2022).

The SD method is predicated on establishing statistical relationships between atmospheric variables in reanalyzed datasets and those measured at meteorological stations (Maraun et al., 2010; Nacar et al., 2022). The multivariate adaptive regression splines (MARS) method, known for its successful application in various engineering problem-solving contexts, is also employed in SD studies (Nasseri et al., 2013; Nacar et al., 2022; Şan et al., 2023). The MARS method was preferred in this study due to its good performance. The SD models built with the MARS method are fed with GCM data to generate future projections (Nacar et al., 2022). GCMs are produced with different parameters and at different centers, so they cannot effectively represent every region with equal accuracy. Consequently, a selection process based on specific criteria becomes essential. Opting for a single GCM choice introduces uncertainties, while excessive GCM selections escalate computational demands and complicate interpretation. An ensemble of high-performance models is created to mitigate these challenges after suitable GCMs are chosen for the studied region or point (Bağçaci et al., 2021).

In the scope of this study, the outputs from 14 GCMs were initially downscaled to a regional scale using the MARS-based SD method. Subsequently, four GCMs that exhibited better compatibility with the daily precipitation variable measured at the meteorological station were identified. These four selected GCMs were then ensembled through arithmetic mean. Consequently, the potential impacts of climate change on the monthly total precipitation in Bursa, one of Türkiye's most densely populated provinces, were investigated for the near future (2030-2059) term under the SSP5-8.5 scenario.

2. Study area and methodology

2.1. Study area and data

Bursa Province, which has a coastline along the Sea of Marmara and ranks as the fourth most populous province in Türkiye, covers an area of 10,819 km² (Fig. 1). The Uluabat Lake, within the provincial boundaries, has been designated as a Ramsar area of international significance. Bursa Province experiences a semi-arid Mediterranean climate with elements of a mountainous climate due to Uludağ Mountain (2,538 m), and arid conditions characterize a considerable portion of the year (Akbaş et al., 2020; Katipoğlu, 2022).

Precipitation data of Bursa meteorological station for the term 1979-2014 were obtained from the Turkish State Meteorology Service. Basic statistics for the data are given in Table 1. Reanalysis datasets used in the establishment of SD models were sourced from the European Centre for Medium-Range Weather Forecasts in NetCDF format (URL 1, 2023) and processed using the R software. Coarse-resolution data of the GCMs were retrieved from the sixth phase of the Coupled Model Intercomparison Project (CMIP6) website (URL 2, 2023) and similarly processed using the R software. The independent variables used in establishing SD models, which are present in the ERA5 dataset, are given in Table 2. When selecting these independent variables, care was taken to ensure that the same variables were available in the GCMs. Consequently, the models developed using the atmospheric variables in the ERA5 dataset were later run with independent variables from the GCM datasets to generate future scenario data.

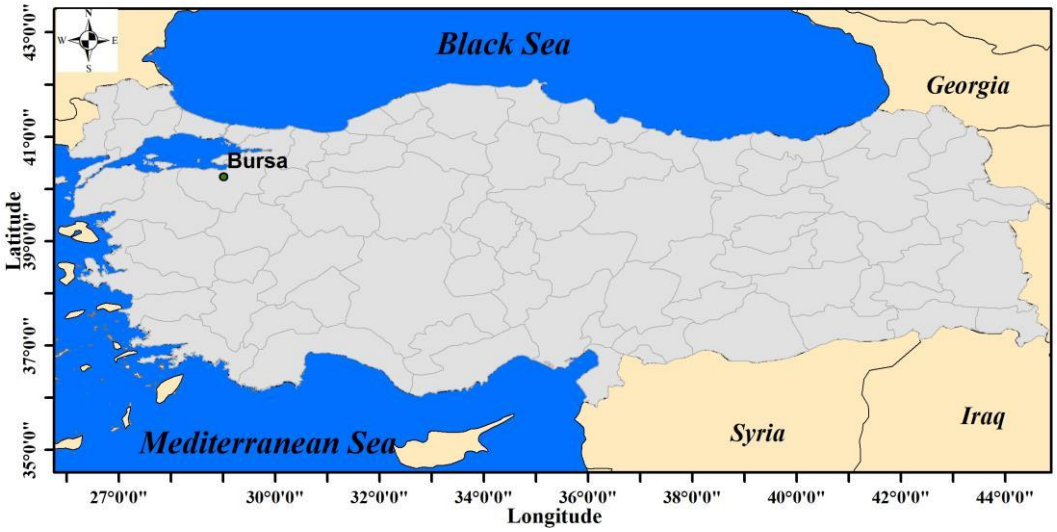


Fig. 1. Location of Bursa meteorological station, Türkiye

Table 1. Basic statistics for the annual total precipitation data of Bursa meteorological station for the years 1979-2014

Mean (mm)	Standard deviation (mm)	Skewness	Kurtosis	Mean wet day
715.42	148.96	1.93	8.58	80.60

Table 2. Independent atmospheric variables used in statistical downscaling models

Variable	Abbreviation	Pressure level (hPa)	Variable	Abbreviation	Pressure level (hPa)
Geopotential height	z	500, 700, 850	Mean air temperature	tm	Surface, 500, 700, 850
Relative humidity	r	500, 700, 850	Sea level pressure	slp	Surface
Meridional wind velocity	u	500, 700, 850	Total precipitation	tp	Surface
Zonal wind velocity	v	500, 700, 850			

2.2. Methodology

To downscale the GCM outputs to a regional scale, MARS-based SD models were established using independent variables from the ERA5 reanalysis dataset and the observed precipitation variables from Bursa meteorological station, as detailed in the study by Şan et al. (2023). In this study, the independent variables used to establish SD models were obtained from selected GCMs from the CMIP6 archive. A total of 14 GCMs having the variables used in the SD models and present in the ERA5 dataset were identified, and their data were downloaded and processed from the respective websites. The names and resolutions of these GCMs are provided in Table 3. Subsequently, the independent variables from these GCMs were designated as inputs to the SD models developed using the ERA5 dataset, and historical precipitation data from these GCMs were generated. The agreement between the generated precipitation data and the observed precipitation values was evaluated using the Kling-Gupta efficiency (KGE) (Gupta et al., 2009; Kling et al., 2012), and the models exhibiting the highest performance were identified. The KGE was calculated as follows:

$$KGE = 1 - \sqrt{\left(\frac{\bar{u}_m}{\bar{u}_o} - 1\right)^2 + \left(\frac{cv_m}{cv_o} - 1\right)^2 + (\rho(o,m) - 1)^2} \quad (1)$$

where $\bar{u}_o$ $(\bar{u}_m), cv_o(cv_m),$ and $\rho(o,m)$ are the arithmetic mean, coefficient of variation, and correlation of the observed (modeled) values, respectively. The closer the KGE value is to 1 within the range of (-∞, 1], the higher the model performance. Subsequently, the first four GCMs with the highest performance values were selected to generate the future term precipitation data. The independent variables associated with these models were designated as new inputs for the SD models, and future socio-economic scenario data were generated. In conjunction with observed precipitation values, these generated future term scenario data were utilized to establish a MARS-based model, and ensemble averages were calculated. It should be noted that GCMs may contain biases arising from parameter optimization, land-sea-atmosphere feedback, and inaccuracies in representing physical-climatic processes (Nahar et al., 2017). For these reasons, the quantile delta mapping (Cannon et al., 2015), a method providing bias correction for averages and outliers (Gümüş et al., 2023), was applied. Then, improved visualization of innovative trend analysis (IV-ITA) for high and low group trends (Güçlü, 2020) and the innovative trend significance test (ITST) for monotonic trends (ITST) (Şen, 2017) were used. Details of these methods can be accessed in the studies by Acar et al. (2022) and Körük et al. (2023).

Table 3. The geneal circulation models obtained from the CMIP6 archive and their resolutions

GCM	Resolution	GCM	Resolution
ACCESS-CM2	1.87° × 1.25°	IPSL-CM6A-LR	1.26° × 2.50°
CanESM5	2.81° × 2.81°	MIROC6	1.40° × 1.40°
CESM2-WACCM	1.30° × 0.90°	MPI-ESM1-2-HR	0.94° × 0.94°
EC-Earth3	0.35° × 0.35°	MPI-ESM1-2-LR	1.90° × 1.90°
FGOALS-g3	2.00° × 2.00°	MRI-ESM2-0	1.10° × 1.10°
INM-CM4-8	2.00° × 1.50°	NorESM2-LM	2.50° × 1.89°
INM-CM5-0	2.00° × 1.50°	NorESM2-MM	0.94° × 1.25°

3. Results and discussion

The KGE values calculated between the precipitation values recorded at the Bursa meteorological station and the downscaled historical scenario data obtained from 14 GCMs are given in Table 4, in which the models with the highest performance values, namely MPI-ESM1-2-LR, INM-CM5-0, CESM2-WACCM, and MPI-ESM1-2-HR, were selected for generating future scenario data. Ensemble averaging was performed on the output precipitation variables of the mentioned GCMs to reduce potential uncertainties. The biases of the obtained outputs were corrected using the quantile delta mapping method. The biases, both corrected and uncorrected for Bursa meteorological station, and the empirical cumulative distribution function graph for the observation data are shown in Fig. 2.

Table 4. Observed precipitation prediction performance rankings of general circulation models

GCM	KGE value	KGE ranking	GCM	KGE value	KGE ranking
MPI-ESM1-2-LR	0.006	1	MIROC6	−0.022	8
INM-CM5-0	−0.006	2	NorESM2-MM	−0.022	9
CESM2-WACCM	−0.007	3	CanESM5	−0.023	10
MPI-ESM1-2-HR	−0.009	4	MRI-ESM2-0	−0.026	11
NorESM2-LM	−0.013	5	IPSL-CM6A-LR	−0.027	12
EC-Earth3	−0.020	6	FGOALS-g3	−0.030	13
INM-CM4-8	−0.020	7	ACCESS-CM2	−0.032	14

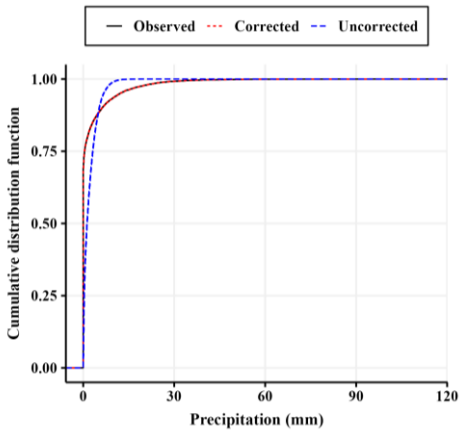


Fig. 2. The bias correction results for the historical (1979-2014) scenario of daily precipitation values, Bursa meteorological station, Türkiye

Table 5. Monthly total precipitation averages and changes for the near past (1979-2014) and near future (2030-2059)

	Jan	Feb	Mar	Apr	May	Jun	Jul	Aug	Sep	Oct	Nov	Dec
Near past	84.7	72.4	67.8	66.7	43.7	38.0	20.1	14.3	40.8	80.4	81.2	101.3
Near future	72.8	59.2	58.5	55.7	43.1	28.4	22.3	13.6	32.8	69.2	62.3	77.7
Change (mm)	−11.8	−13.1	−9.3	−10.9	−0.7	−9.6	2.2	−0.8	−8.0	−11.2	−18.9	−23.5
Change (%)	−14.0	−18.2	−13.7	−16.4	−1.5	−25.2	10.9	−5.4	−19.6	−13.9	−23.2	−23.2

Table 6. High and low group and monotonic trend results (the cells highlighted with white denote non-significant trend)

Method	Term	Group	Jan	Feb	Mar	Apr	May	Jun	Jul	Aug	Sep	Oct	Nov	**Dec**
ITST	NP		−0.4	1.7	1.4	0.6	−0.3	0.4	−0.1	0.3	1.5	1.7	−0.7	0.7
slope (mm/month)	NF		1.3	−2.0	0.8	0.8	−0.3	−0.3	−0.7	−0.8	−1.3	−2.4	1.5	
IV-ITA Change	NP	Low	17.7	30.9	154.5		−17.4		−18.1	11.1	330.2		−7.5	
(%)		High	−13.3	64.6	10.4	25.9	−13.0	28.4	−11.7	51.8	84.3	69.5	−15.6	20.8
		All	−7.6	53.8	44.8	18.4	−13.4	22.8	−12.0	49.5	98.7	48.6	−14.0	13.2
	NF	Low	−37.1	−39.2	44.9	18.5	−34.5	41.3	−93.6	−100.0	−34.5	−61.6	41.4	−10.2
		High	52.5	−41.3		26.4		−28.0	−36.3	−61.3	−48.8	−39.4	46.8	18.9
		All	29.9	−40.0	23.7	23.2	−10.7	−15.8	−38.5	−62.6	−46.5	−41.2	45.1	

NP, near past; NF, near future

It is clear from Fig. 2, that bias correction has effectively reduced the bias in low and moderate precipitation values while maintaining acceptable levels of bias correction in high precipitation values. The bias correction procedure applied to the historical data has also been extended to the future SSP5-8.5 scenario outputs, addressing potential biases in the future data. Daily precipitation in the future term has been converted into monthly total precipitation, and then intra-term averages and changes are given in Table 5.

Compared to the recent past, an average of 14% decrease is expected in monthly precipitation in the near future. The biggest decrease is predicted in December, with 23.5 mm. While no notable change is projected between May and September, a decrease of approximately 18% is expected in other months. Intra-term ITST monotonic trends are given in Table. 6, and intra-term IV-ITA high and low group trends are given in Table 6 and Fig. 4.

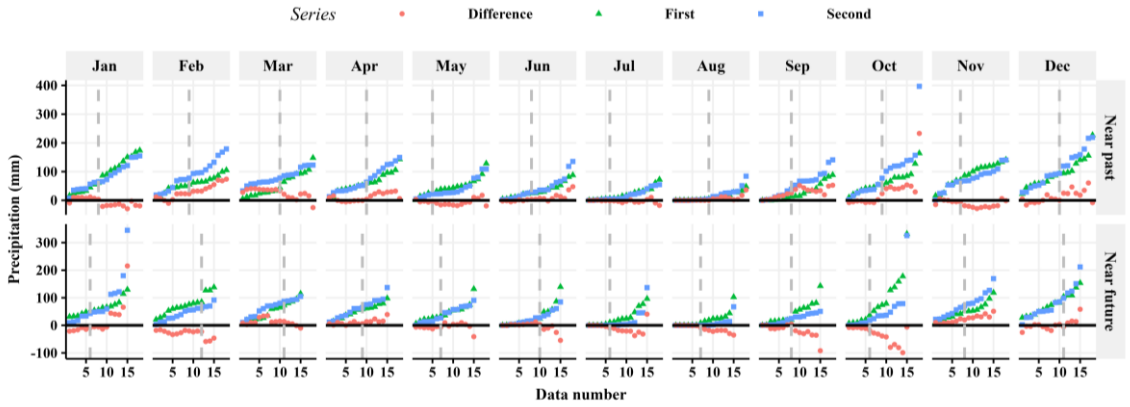


Fig. 4. IV-ITA results of monthly total precipitation (vertical grey dashed lines: change point in difference series)

In the months except for March and April (increasing), May and July (decreasing), near past and near future trend directions are different from each other (Table. 6). While there is a decreasing trend in the near past in January and November, an increasing trend is expected in the near future. Still, the opposite situation is expected in February, July, August, September, and October. All trend results of the IV-ITA method are also in the same direction as the ITST method results (Table 6 and Fig. 4). While an increasing trend is observed in the range of 11-50% (28-84%) of low (high) values in January, February, August, and September (February, June, August, September, and October) during the near past, a decreasing trend is predicted in the range of 34-100% (28-61%) in the near future. There is a high variation between −100 and 330% in August and September, and the reason is the low average precipitation values. In the near past, there is no trend in the low group in April, June, October, and December, but there is an increase in the high group and all trends. In the near future, there is a low and all increasing (decreasing) trend in March (May), a decreasing trend in the low group, and an increasing trend in the high group in December, but there is no all trend. In addition, in the near past, in January, the increasing trend at low values and the decreasing trend at high values turned into a decrease in all trends.

4. Conclusions

In this study, alongside the variations in monthly total precipitation of Bursa Province, intraterm monotonic and group trends have been examined in the near past (1979-2014) and the near future under the SSP5-8.5 scenario (2030-2059). When a 14% decrease is predicted in monthly precipitation in the near future, a significant decrease is expected in other months except for May-September, and the most considerable

decrease is projected in December. It is predicted that there may be different trends between the near past and the near future in other months except for March-May and July. It can be inferred from May-April, October, and December that the trends in high and low groups may not consistently in the same direction and may not always have an impact on all trends. Thus, it is recommended that since the behavior of group trends in trend analysis may be different from the monotonic trend, using them together may be preferred for careful preparation of water resources plans.

Declaration of conflicting interests

The authors declared no potential conflicts of interest with respect to the research, authorship, and/or publication of this article.

References

Acar E, Kankal M, Akçay F, Şan M (2022) Innovative polygon trend analyses with star graph for rainfall and temperature data in agricultural regions of Turkey. Environmental Earth Sciences 81(23):530.

Ahmed K, Shahid S, Nawaz N (2018) Impacts of climate variability and change on seasonal drought characteristics of Pakistan. Atmospheric Research 214:364–374.

Akbaş A, Freer J, Ozdemir H, Bates PD, Turp MT (2020) What about reservoirs? Questioning anthropogenic and climatic interferences on water availability. Hydrological Processes 34(26):5441–5455.

Bağçacı SÇ, Yücel İ, Düzenli E, Yılmaz MT (2021) Intercomparison of the expected change in the temperature and the precipitation retrieved from CMIP6 and CMIP5 climate projections: A Mediterranean hot spot case, Turkey. Atmospheric Research 256:105576.

Cannon AJ, Sobie SR, Murdock TQ (2015) Bias correction of GCM precipitation by quantile mapping: how well do methods preserve changes in quantiles and extremes? Journal of Climate 28(17):6938–6959.

Diffenbaugh NS, Giorgi F (2012) Climate change hotspots in the CMIP5 global climate model ensemble. Climatic Change 114(3–4):813–822.

Ekstrom M, Grose MR, Whetton PH (2015) An appraisal of downscaling methods used in climate change research. Wiley Interdisciplinary Reviews: Climate Change 6(3)301–319.

Güçlü YS (2020) Improved visualization for trend analysis by comparing with classical Mann-Kendall test and ITA. Journal of Hydrology 584:124674.

Gümüş B, Oruç S, Yücel İ, Yılmaz MT (2023) Impacts of climate change on extreme climate indices in Türkiye driven by high-resolution downscaled CMIP6 climate models. Sustainability 15(9):7202.

Gupta HV, Kling H, Yilmaz KK, Martinez GF (2009) Decomposition of the mean squared error and NSE performance criteria: Implications for improving hydrological modeling. Journal of Hydrology 377(1–2):80–91.

Katipoğlu OM (2022) Analyzing the trend and change point in various meteorological variables in Bursa with various statistical and graphical methods. Theoretical and Applied Climatology 150(3–4):1295–1320.

Keupp L, Hertig E, Kaspar-Ott I, Pollinger F, Ring C, Paeth H, Jacobeit J (2019) Weighted multi-model ensemble projection of extreme precipitation in the Mediterranean region using statistical downscaling. Theoretical and Applied Climatology 138(3–4):1269–1295.

Kling H, Fuchs M, Paulin M (2012) Runoff conditions in the upper Danube basin under an ensemble of

climate change scenarios. Journal of Hydrology 424–425:264–277.

Körük AE, Kankal M, Yıldız MB, Akçay F, Şan M, Nacar S (2023) Trend analysis of precipitation using innovative approaches in northwestern Turkey. Physics and Chemistry of the Earth Parts A/B/C 131:103416.

Maraun D, Wetterhall F, Ireson AM (2010) Precipitation downscaling under climate change: recent developments to bridge the gap between dynamical models and the end user. Reviews of Geophysics 48(3):RG3003.

Nacar S, Kankal M, Okkan U (2022) A downscaling application for local meteorological variables of Eastern Black Sea Basin and scenario-based predictions. Teknik Dergi 33(6):12877–12911.

Nahar J, Johnson F, Sharma A (2017) Assessing the extent of non-stationary biases in GCMs. Journal of Hydrology 549:148–162.

Nasseri M, Tavakol-Davani H, Zahraie B (2013) Performance assessment of different data mining methods in statistical downscaling of daily precipitation. Journal of Hydrology 492:1–14.

Şan M, Nacar S, Kankal M, Bayram A (2023) Daily precipitation performances of regression-based statistical downscaling models in a basin with mountain and semi-arid climates. Stochastic Environmental Research and Risk Assessment 37(4):1431–1455.

Şen Z (2017) Innovative trend significance test and applications. Theoretical and Applied Climatology 127(3–4):939–947.

URL 1 (2023). Climate Data Store. Available online: https://cds.climate.copernicus.eu/cdsapp#!/search?type=dataset.

URL 2 (2023). WCRP Coupled Model Intercomparison Project (Phase 6). Available online: https://esgf-node.llnl.gov/search/cmip6/